Mitochondrion 36 (2017) 60–65

Contents lists available at ScienceDirect

Mitochondrion

journal homepage: www.elsevier.com/locate/mito

Optical coherence tomography angiography of the peripapillary retina and optic nerve head in dominant optic atrophy

Nicole Balducci [a,*], Antonio Ciardella [b], Roberto Gattegna [c], Qienyuan Zhou [d], Maria Lucia Cascavilla [g], Chiara La Morgia [e,f], Giacomo Savini [c], Vincenzo Parisi [c], Francesco Bandello [g], Valerio Carelli [e,f], Piero Barboni [a,g]

[a] Studio Oculistico d'Azeglio, Piazza Galileo, 6, 40123 Bologna, Italy
[b] Ophthalmology Unit, Policlinco Sant'Orsola-Malpighi, Via Palagi, 9, 40138 Bologna, Italy
[c] GB Bietti Foundation IRCCS, Via Livenza, 3, 00128 Rome, Italy
[d] Optovue, Inc., 2800 Bayview Drive, Fremont, CA 94538, USA
[e] Unit of Neurology, Department of Biomedical and Neuromotor Sciences (DIBINEM), University of Bologna, Via Altura, 3, 40139 Bologna, Italy
[f] IRCCS, Istituto delle Scienze Neurologiche di Bologna, Ospedale Bellaria, Via Altura, 3, 40139 Bologna, Italy
[g] Scientific Institute San Raffaele, Via Olgettina, 60 Milan, Italy

ARTICLE INFO

Article history:
Received 14 June 2016
Received in revised form 8 February 2017
Accepted 6 March 2017
Available online 10 March 2017

Keywords:
Dominant optic atrophy
DOA
Optical coherence tomography angiography
Vessel density
Inherited mitochondrial optic neuropathies

ABSTRACT

Peripapillar and nerve head vessel density (VD) was measured in 10 patients affected by Dominant optic atrophy (DOA) using optical coherence tomography angiography (OCT-A) and compared to the measurements of 15 age- and gender-matched controls.
DOA patients showed VD reduction, mostly in the temporal and inferotemporal peripapillary sectors, according to the preferential involvement of the papillomacular bundle. Despite poor best-corrected visual acuity (BCVA), OCT-A revealed good repeatability. VD correlated with functional (mean deviation of visual field and BCVA) and structural (retinal nerve fiber layer thickness) parameters and could be a non-invasive, quantitative tool for the monitoring of the disease and of the therapeutic approaches.

1. Introduction

Dominant optic atrophy (DOA) is a genetically determined mitochondrial optic neuropathy, characterized by slowly progressive bilateral visual loss, cecocentral scotoma, impairment of color vision, and temporal or diffuse atrophy of the optic disc. The disease has incomplete penetrance and variable expressivity, ranging from subclinical manifestations to legal blindness (Kjer, 1959; Newman, 2005; Yu-Wai-Man et al., 2010; Cohn et al., 2008).

Most cases of DOA have been associated with mutations in the OPA1 gene on the long arm of chromosome 3q28–q29, which encodes a dynamin-related GTPase targeted to mitochondria (Yu-Wai-Man et al., 2011). It has been previously suggested that OPA1, by regulating apoptosis, may participate to the modeling of the eye during development (Yarosh et al., 2008), contributing to determine the number of retinal ganglion cells and the optic nerve head (ONH) conformation at birth (Barboni et al., 2010).

The microvascular involvement is a typical feature of some mitochondrial diseases, such as Leber hereditary optic neuropathy (LHON) (Nikoskelainen et al., 1983) and Mitochondrial Myopathy, Encephalopathy, Lactic Acidosis, and Stroke-Like Episodes (MELAS).

To date, a new promising optical coherence tomography (OCT) technology, called OCT-angiography (OCT-A) can provide information on retinal blood perfusion. Using the split-spectrum amplitude-decorrelation angiography (SSADA) algorithm, ONH and peripapillary perfusion can be quantified (Jia et al., 2012a). Using OCT-A a reduction of ONH and peripapillary perfusion has been quantified in optic neuropathies, such as in glaucoma (Liu et al., 2015; Wang et al., 2015; Holló, 2016; Rao et al., 2016a; Rao et al., 2016b; Yarmohammadi et al., 2016) and in multiple sclerosis (Wang et al., 2014).

To our knowledge, currently only little information is available on vascular supply in DOA (Inoue et al., 2016; Gränse et al., 2003; Rönnbäck et al., 2014). This may add to our understanding of DOA pathophysiology, and be useful to monitor disease progression in clinical practice and, ultimately, to assess the effectiveness of new therapeutic approaches.

The purpose of this study was to measure the peripapillary and ONH microcirculation in DOA patients compared to healthy control, and to correlate these perfusion indexes with the functional and anatomical conventional assessments, such as visual field (VF) and structural OCT.

Abbreviations: ONH, optic nerve head; VD, vessel density; N, nasal; IN, inferonasal; IT, inferotemporal; T, temporal; IT, inferotemporal; IN, inferonasal.

* Corresponding author.
E-mail address: balduccinicole@gmail.com (N. Balducci).

http://dx.doi.org/10.1016/j.mito.2017.03.002
1567-7249/

2. Material and methods

2.1. Study population

This prospective, cross-sectional, observational study enrolled 10 patients affected by molecularly confirmed DOA with OPA1 heterozygous mutation from 7 unrelated pedigrees and 15 controls.

All subjects had extensive ophthalmological examinations including best-corrected visual acuity (BCVA), axial length (AL, Aladdin, Topcon Europe, Visia Imaging, San Giovanni Valdarno, Arezzo, Italy), mean deviation (MD) of VF (SITA standard 30-2, Humphrey VF analyzer, HFA II 750-4.1 2005; Carl Zeiss Meditec, Dublin, CA, USA), macular ganglion cell-inner plexiform layer (GC-IPL) and peripapillar retinal nerve fiber layer (RNFL) thickness using spectral domain-OCT (Cirrus HD-OCT, software V.6.0; Carl Zeiss Meditec, Inc., Dublin, CA, USA).

Exclusion criteria for DOA patients were the presence of any retinal or optic nerve disease other than DOA, and spherical or cylindrical refractive errors higher than 4 and 2 diopters (D), respectively.

Inclusion criteria for control group were the following: BCVA of at least 0.8 (decimal fraction); spherical or cylindrical refractive errors <4 and 2 diopters (D), respectively; intraocular lens pressure (IOP) < 21 mm Hg; normal appearance of the optic disc; normal VF and no any ocular or systemic disease that could interfere with OCT-A examination.

All participants gave their informed consent according to the Declaration of Helsinki. The study was approved by the internal review board at the Department of Neurological Sciences, University of Bologna.

2.2. Instrumentation and procedure

OCT-A scans were obtained by spectral domain OCT system (AngioVue Imaging System; Optovue, Inc., software version 2015.100.0.33 Fremont, CA, USA). This system has an A-scan rate of 70 kHz per second, using a light source centered on 840 nm and a bandwidth of 45 nm. The tissue resolution was 5 μm axially for OCT scans and 15 μm for OCT-A scans. Both eyes of each participant were examined and scanned at least twice within the same visit. Before imaging, each subject's pupils were dilated with a combination of 0,5% tropicamide and 10% phenylephrine. An internal fixation light was used to center the scanning area. The OCT signal position and signal quality were optimized by means of "Auto All" function, which performs in sequence the "Auto Z" to find the reference position for obtaining the retina OCT image, the "Auto F" to find the focus for the particular subject refraction, and the "Auto P" to find the polarization match for the particular subject ocular polarization. Each image set comprised 2 raster volumetric patterns (one vertical priority and one horizontal priority) covering 4.5 × 4.5 mm centered on the optic nerve head. An orthogonal registration algorithm was used to produce merged 3- dimensional OCT angiograms with reduced motion artifacts and improved signal-to-noise ratio (SNR) (Kraus et al., 2014). Each volume was composed of a raster of 304 B-scans with each B-scan consisting of two consecutive repeats. Each B-scan contained 304 A-scans. The SSADA algorithm compares the two consecutive B-scans at the same location to detect flow using motion contrast (Jia et al., 2014).

The peripapillary region was defined as a 700-μm-wide elliptical annulus extending from the optic disc boundary. An en face angiogram of the retinal circulation was obtained by the maximum flow (decorrelation value) projection of all points alone a given A-scan within the range of the en face slab. The optic disc boundary was detected automatically by software based on Bruch's membrane opening. In the case where disc margin detection error was observed, manual correction of the disc margin was performed by the observer.

Peripapillary and ONH vessel density (VD) was defined as the percentage area occupied by the large vessels and microvasculature in the peripapillar and optic disc region, respectively.

Scans with low quality (i.e. if the subject blinked or if there were motion artifacts in the data set) and signal strength index (SSI) <50 were excluded and repeated until at least 2 good quality scans were achieved.

2.3. Vascular layer segmentation

Vascular retinal layers were visualized and segmented. Two different layer settings (Fig. 1) were calculated by the software:

1) Optic nerve head (ONH) layer setting: 150 μm thick slab following ILM surface contour in order to evaluate optic nerve head vascularization (whole and temporal), supplied by short posterior ciliary arteries and including great vessels emergences. (Fig. 1, top line). Whole and temporal ONH VD was evaluated.
2) Radial peripapillar capillary (RPC) layer setting: from ILM to RNFL posterior boundary to evaluate superficial peripapillar vessels, running parallel to RNFL and supplied by central retinal artery (Fig. 1, bottom line). Whole and sectorial (temporal, superotemporal, superonasal, nasal, inferonasal and inferotemporal) RPC VD was evaluated.

Two investigators checked segmentation quality before testing vessel density.

2.4. Statistical analysis

Values were presented as median and range. BCVA was converted into the logarithm of the minimum angle of resolution (LogMAR) units for the statistical analysis. Because of the small sample size, data were analyzed by non-parametric tests. Mann-Whitney test was used for VD comparison between DOA patients and controls. Spearman rank correlation test was used to investigate the correlation between VD and age, AL, BCVA, MD of VF, disc area, rim area, cup/disc (C/D) ratio, RNFL and GC-IPL thickness. Multiple linear regression analysis was performed to determine independent variables affecting VD. Sensitivity analysis was carried out using area under the receiver operator characteristic (AUROC). Within-visit repeatability of VD was calculated with 2 sets of images obtained at a single visit. Variability of each parameter in DOA patients was assessed by the coefficient of variation (CoV), calculated as the root-mean-square measurement variation divided by the mean of the measured values.

Statistical significance was assumed for p values <0.05. MedCalc V.13.0.4.0 (MedCalc, Mariakerke, Belgium) was used for statistical analysis.

3. Results

3.1. Study population

OCT-A was performed in 20 eyes of 10 DOA patients and 15 eyes of 15 controls, matched for eye, gender and AL. Demographic and clinical characteristics of patients and controls were summarized in Table 1. At least 3 measurements (median 4.5, range 3–6) per eye were performed in DOA patients in order to obtain at least 2 acceptable images (SSI > 50 and no motion artifacts) due to low fixation. However, no patient or control was excluded for poor quality images.

3.2. Comparison of VD

A dense microvascular network around (Fig. 2, top left) and inside the disc (Fig. 2, bottom left) was visible in controls with OCT-A. Indeed, Figs. 2 (top and bottom right) shows the typical attenuation of the vascular network in the RPC and in the ONH, respectively, found in DOA patients.

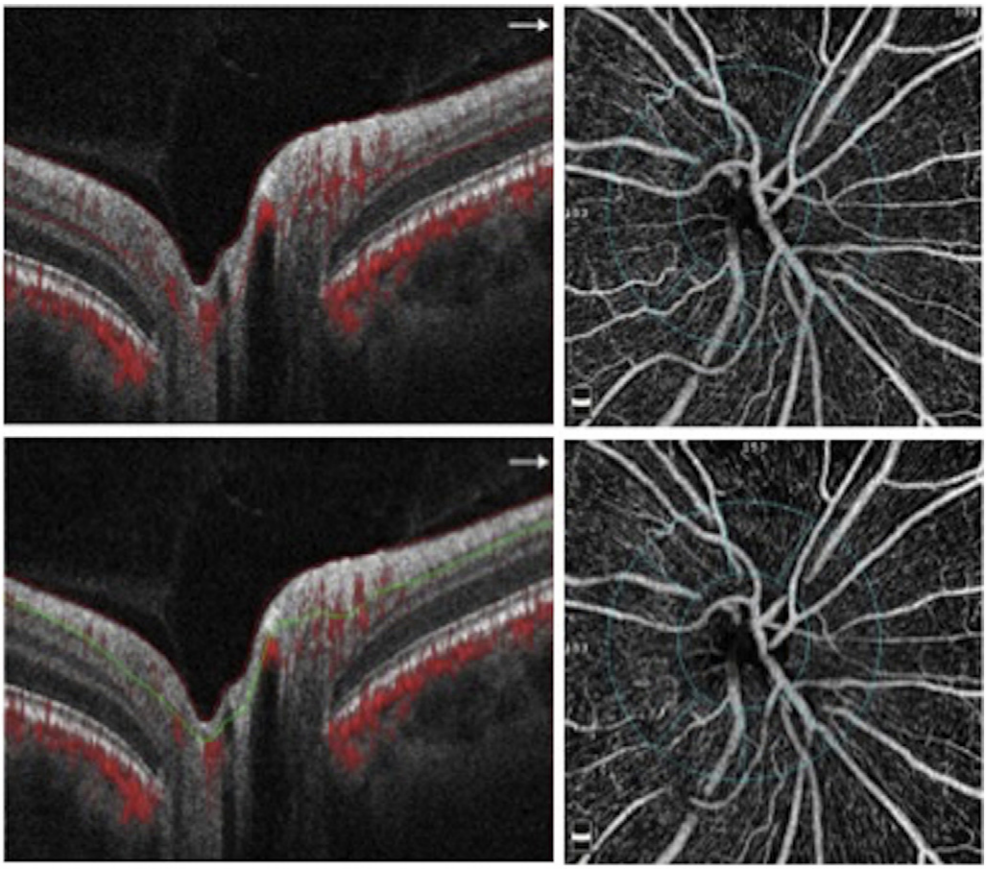

Fig. 1. Vascular retinal layers segmentation. Optical coherence tomography (OCT, top left and bottom left) and optical coherence tomography angiography (OCT-A, top right and bottom right) of a control's right eye. Note the different layer segmentation (red line for optic nerve head layer and green line for radial peripapillar capillary layer on OCT image) and the different vascular visualization with OCT-A. Note the blue circles superimposed to the optic nerve head, representing the optic nerve boundary (inner circle) and the peripapillar sectors (outer circle).

Table 2 shows RPC and ONH VD analyzed in DOA patients and controls. Mann-Whitney test revealed statistically significant VD reduction in DOA group for all the variables analyzed, except for whole ONH VD.

3.3. Sensitivity analysis

All the parameters, except whole ONH VD were highly sensitive to distinguish DOA patients from controls (Table 3). Specifically, AUROC curves revealed the highest values (AUROC = 1) for whole, temporal and inferotemporal RPC VD.

Table 1
Clinical data of patients affected by Dominant Optic Atrophy (DOA) and controls.

	DOA ($n = 20$) Median (range)	Control ($n = 15$) Median (range)	P value*
Age (years)	38.5 (15 to 66)	40 (16 to 66)	ns
Sex (male:female)	7:3	6:9	ns**
AL (mm)	24.06 (23.18 to 26.36)	23.93 (22.1 to 26.04)	ns
BCVA (LogMAR)	0.4 (0.1 to 1)	−0.01 (0.0 to −0.1)	<0.0001
GC-IPL average (μm)	50 (44 to 66)	82 (73 to 96)	<0.0001
RNFL average (μm)	65 (51 to 71)	93 (81to 127)	<0.0001
MD (dB)	−4.01 (−10.2 to −1.64)	0.16 (0.18 to −0.05)	<0.0001
Disc area (mm^2)	1.62 (0.89 to 2.18)	1.9 (1.41 to 2.47)	0.0005
Rim area	1.11 (0.74 to 1.71)	1.35 (0.95 to 2.12)	0.001
C/D ratio	0.56 (0.12 to 0.74)	0.52 (0.06 to 0.77)	ns

BCVA: best-corrected visual acuity; LogMAR: logarithm of the minimum angle of resolution, GC-IPL: macular ganglion cell-inner plexiform layer thickness; RNFL: retinal nerve fiber layer thickness; MD: mean deviation; C/D: cup/disc; ns: not significant.
* Mann-Whitney test.
** χ^2 test.

3.4. Correlation with functional and anatomical parameters

Table 4 shows correlation data among variables with AUROC = 1. Univariate Spearman correlation analysis showed that whole RPC VD was positively correlated with MD ($r = 0.618$; $p = 0.0063$) and RNFL thickness ($r = 0.66$; $p = 0.0013$). On the contrary, a significant negative correlation was found between whole RPC VD and BCVA ($r = -0.47$; $p = 0.035$) and age ($r = -0.47$; $p = 0.0336$). Moreover, Temporal RPC VD was negatively correlated with BCVA ($r = -0.48$; $p = 0.03$).

No correlations were found between VD parameters and AL, disc area, rim area, C/D ratio or GCC thickness.

Multiple linear regression analysis, in which VD was considered the dependent variable, showed that MD and BCVA were predictors of whole RPC VD ($p = 0.008$ and 0.0017, respectively) and that BCVA was a predictor of temporal RPC VD ($p = 0.0019$).

3.5. VD repeatability

We calculated intra-visit repeatability in DOA patients. The Coefficient of Variations (CoVs) ranged between 3.48% and 8.75%, with the best CoV value detected for whole RPC and the worst one for temporal ONH VD.

4. Discussion

In this study we found that peripapillary and optic nerve head temporal microvascular network were reduced in DOA patients.

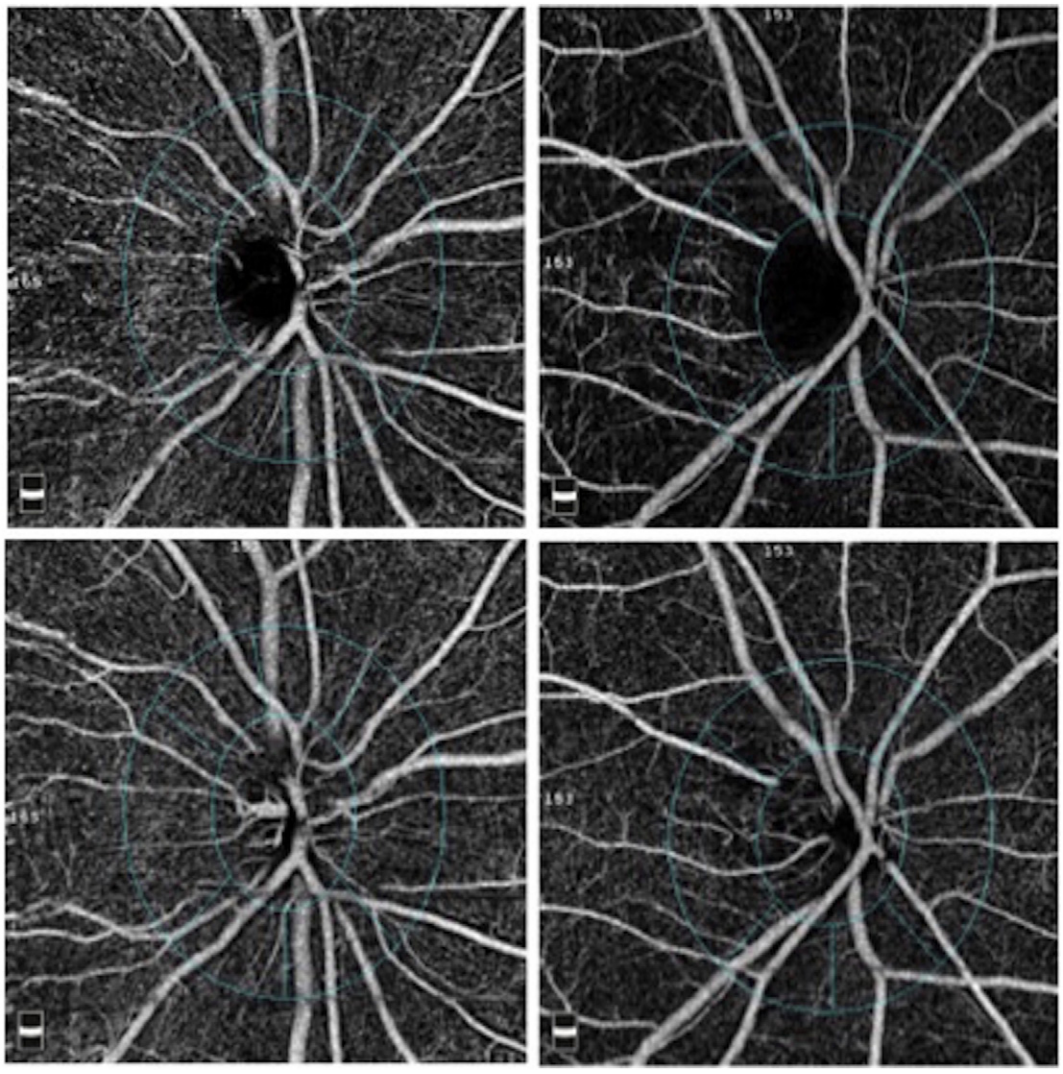

Fig. 2. OCT-A in control subject and Dominant Optic Atrophy (DOA) patient. Visualization of radial peripapillary capillaries (RPC, top images) and optic nerve head (ONH, bottom images) microvasculature in a control subjects (left images) and in a DOA patient (right images).

We designed this study to first analyze the microvasculature derived from the central retinal artery by evaluating the superficial peripapillar VD (whole and sectorial) at the level of the RPC. In addition, we also studied the blood supply from short posterior ciliary arteries by assessing temporal ONH VD at a thicker setting (150 μm), which seems to capture the vasculature in the prelaminar tissue layer. Finally, in order to exclude the influence of great vessels we only evaluated the temporal ONH sector, where no great vessels are detectable. As shown in Fig. 2 the deeper ONH layer setting (bottom images) can detect ONH microvasculature, compared with RPC layer setting (top images). Thus, two different layer settings are necessary to evaluate peripapillary and optic disc microvasculature.

The microvascular network reduction in DOA confirmed studies that evaluated optic nerve head microcirculation using laser speckle flowgraphy (LSFG) (Inoue et al., 2016; Gränse et al., 2003). Moreover, our results showed that RPC VD was diffusely reduced and the most

Table 2
Vessel density in DOA and control group.

VD (%) Median (range)	DOA $n = 20$	Control $n = 15$	*P* value*
Whole RPC	45.52 (35.59 to 49.12)	63.29 (57.3 to 67.7)	<0.0001
N-RPC	48.38 (36.61 to 55.45)	60.25 (51.87 to 65.35)	<0.0001
IN-RPC	48.80 (30.8 to 58.2)	64.51 (50.74 to 69.66)	<0.0001
IT-RPC	46.17 (33.1 to 58.44)	68.19 (61.84 to 76.34)	<0.0001
ST-RPC	50.38 (35.97 to 63.75)	65.71 (59.81 to 73.77)	<0.0001
SN-RPC	50.84 (33.43 to 56.62)	60.4 (49.26 to 66.95)	<0.0001
T-RPC	36.85 (24.97 to 41.39)	63.56 (56.46 to 69.47)	<0.0001
Whole ONH	51.71 (37.99 to 60.19)	53.79 (43.92 to 58.49)	ns
T-ONH	36.46 (21.25 to 48.18)	48.37 (35.98 to 60.7)	<0.0001

DOA: dominant optic atrophy; SD: standard deviation; VD: vessel density; RPC: retinal peripapillar capillaries; N:nasal; IN: inferonasal; IT: inferotemporal; ST: superotemporal; SN: superonasal; T: temporal; ONH: nerve head.
* Mann-Whitney test.

Table 3
Area under the receiver operator characteristic (AUROC) curves to detect vessel density reduction.

Parameter	AUROC curve	95% CI
Whole RPC	1	0.900–1.000
N-RPC	0.990	0.882–1.000
IN-RPC	0.970	0.849–0.999
IT-RPC	1	0.900–1.000
ST-RPC	0.957	0.828–0.997
SN-RPC	0.920	0.777–0.984
T-RPC	1	0.900–1.000
Whole ONH	0.573	0.395–0.738
T-ONH	0.92	0.777–0.984

N:nasal; IN: inferonasal; IT: inferotemporal; ST: superotemporal; SN: superonasal; T: temporal; ONH: nerve head.

Table 4
Correlation between VD and functional and anatomical parameters.

	Age	BCVA	AL	MD	RNFL	GC-IPL	Disc area	Rim area	C/D ratio
Whole-RPC	$p = 0.033$ $r = -0.46$	$p = 0.035$ $r = -0.47$	ns	$p = 0.0007$ $r = 0.61$	$p = 0.0013$ $r = 0.66$	ns	ns	ns	ns
IT-RPC	ns	ns	ns	ns	ns	ns	ns	ns	ns
T-RPC	ns	$p = 0.03$ $r = -0.48$	ns	ns	ns	ns	ns	ns	ns

Univariate Spearman correlation analysis.
VD: vessel density; RPC: retinal peripapillar capillaries; IT: inferotemporal; T: temporal; BCVA: best-corrected visual acuity; AL: axial length; MD: mean deviation; RNFL: retinal nerve fiber layer: GC-IPL: macular ganglion cell-inner plexiform layer; C/D: cup/disc.

sensitive parameters, able to distinguish DOA from controls (AUROC = 1), were the whole, temporal and infero-temporal peripapillar sectors. These findings fit the preferential involvement of the small axons of the papillomacular bundle in DOA, which hallmarks also other mitochondrial optic neuropathies (Carelli et al., 2004). These results differ from findings in glaucoma (Holló, 2016; Rao et al., 2016a), where greater VD reduction and higher sensibility were found in the superotemporal and mostly in the inferotemporal sector, rather than in the temporal, confirming the different pathogenesis and pattern of fiber/vascular involvement in the two diseases.

ONH VD analysis demonstrated a significant reduction of temporal sector and no reduction of whole VD compared with controls. Differently, in glaucoma and in multiple sclerosis VD reduction involved both temporal (Jia et al., 2012b) and whole ONH assessment (Wang et al., 2015; Jia et al., 2012b; Wang et al., 2014; Rao et al., 2016b), although also in glaucoma ONH VD was less sensitive than RPC to differentiate glaucoma patient from control (Rao et al., 2016b). The small optic disc size in DOA (Barboni et al., 2011), and the emergency of great disc vessels could influence these results. Moreover, ONH layer may include more or less retinal layers and their associated vessel networks depending on the eye anatomy and this could influence the variability across subjects. A better definition of ONH layer is needed to assess full retinal vasculature in the optic nerve head region. Our hypothesis is that in DOA there is a prevalent impairment of both peripapillary capillary derived from central retinal artery, and temporal ONH capillary from posterior ciliary arteries. This scenario is corroborated by recent studies in DOA, showing reduced diameter of central retinal vessels (Rönnbäck et al., 2014) and reduced end diastolic velocities, as well as increased resistive index by Color Doppler measurements (Gränse et al., 2003).

Despite poor BCVA and fixation in DOA patients, OCT-A revealed good repeatability, as the COV ranged from 3.48% and 8.75%. These results were similar to previous studies of OCT-A in glaucoma (Liu et al., 2015; Wang et al., 2015, Jia et al., 2012a, 2012b) and better than other non-invasive techniques, such as laser Doppler flowmetry (LDF) and LSFG (Yaoeda et al., 2000; Jonescu-Cuypers et al., 2004) We suggested that OCT-A could be a useful tool for monitoring disease and for inter-individual comparisons.

In DOA group, whole RPC VD strongly correlated with functional (MD and BCVA) and structural parameters (RNFL thickness). Age also slightly correlated with whole RPC VD ($p = 0.03$) and consequently with the disease duration. Multiple linear regression analysis showed that MD and BCVA were predictors of whole RPC VD, and BCVA was a predictor of temporal RPC VD. Thus, potentially the perfusion indexes may be useful for staging and monitoring DOA and for understanding the different phenotypic expressivity.

In recent glaucoma studies peripapillary VD was correlated with MD, but not with RNFL thickness (Liu et al., 2015; Yarmohammadi et al., 2016), and optic disc VD was correlated with MD, RNFL and GC-IPL thickness (Wang et al., 2015). Larger studies are necessary to carefully establish correlations between VD and functional and structural parameters.

In DOA patients, as in glaucoma, we are not able to determine if the vessel damage is primary or secondary to the fiber reduction, due to the slow progression of both diseases.

This study has some limitations: the small sample size, including both eyes for each patient, which is due to the rarity of DOA, and the cross-sectional design in consideration to the slow disease progression characterizing DOA.

5. Conclusion

In conclusion, microvascular damage of the optic disc and radial peripapillary capillaries were found in DOA patients. The greater temporal RPC VD reduction compared with controls is in agreement with the preferential involvement of the papillomacular bundle in DOA. OCT-A is a repeatable and non-invasive tool to detect both peripapillary and optic disc microvascular networks also in patients with poor fixation and could be useful to study the vascular component and the consequent optic nerve metabolism in this mitochondrial optic neuropathy. Moreover, global VD correlates with global functional and structural parameters and could be a quantitative parameter for monitoring disease progression and assessment of future therapeutic approaches.

Financial disclosure

The contribution of GB Bietti Foundation IRCCS was supported by the Ministry of Health, Italy and Fondazione Roma. Qienyuan Zhou is an employee of Optovue, Inc.

References

Barboni, P., Carbonelli, M., Savini, G., et al., 2010. OPA1 mutations associated with dominant optic atrophy influence optic nerve head size. Ophthalmology 117, 1547–1553.
Barboni, P., Savini, G., Parisi, V., Carbonelli, M., La Morgia, C., Maresca, A., Sadun, F., De Negri, A.M., Carta, A., Sadun, A.A., Carelli, V., 2011 Oct. Retinal nerve fiber layer thickness in dominant optic atrophy measurements by optical coherence tomography and correlation with age. Ophthalmology 118 (10), 2076–2080.
Carelli, V., Ross-Cisneros, F.N., Sadun, A.A., 2004. Mitochondrial dysfunction as a cause of optic neuropathies. Prog. Retin. Eye Res. 23 (1), 53–89 Jan.
Cohn, A.C., Toomes, C., Hewitt, A.W., et al., 2008. The natural history of OPA1-related autosomal dominant optic atrophy. Br. J. Ophthalmol. 92 (10), 1333–1336.
Gränse, L., Bergstrand, I., Thiselton, D., Ponjavic, V., Heijl, A., Votruba, M., Andréasson, S., 2003. Electrophysiology and ocular blood flow in a family with dominant optic nerve atrophy and a mutation in the OPA1 gene. Ophthalmic Genet. 24 (4), 233–245.
Holló, G., 2016. Vessel density calculated from OCT angiography in 3 peripapillary sectors in normal, ocular hypertensive, and glaucoma eyes. Eur. J. Ophthalmol. 26 (3): e42–e45. http://dx.doi.org/10.5301/ejo.5000717 Apr 12.
Inoue, M., Himori, N., Kunikata, H., Takeshita, T., Aizawa, N., Shiga, Y., Omodaka, K., Nishiguchi, K.M., Takahashi, H., Nakazawa, T., 2016. The reduction of temporal optic nerve head microcirculation in autosomal dominant optic atrophy. Acta Ophthalmol. http://dx.doi.org/10.1111/aos.12999 Mar 3 (Epub ahead of print).
Jia, Y., Morrison, J.C., Tokayer, J., Tan, O., Lombardi, L., Baumann, B., Lu, C.D., Choi, W., Fujimoto, James G., Huang, D., 2012a. Quantitative OCT angiography of optic nerve head blood flow. Biomed. Opt. Express 3 (12), 3127–3137.
Jia, Y., Tan, O., Tokayer, J., et al., 2012b. Split-spectrum amplitude-decorrelation angiography with optical coherence tomography. Opt. Express 20, 4710–4725.
Jia, Y., Ewi, E., Wang, X., et al., 2014. Optical coherence tomography angiography of optic disc perfusion in glaucoma. Ophthalmology 121 (7), 1322–1332.
Jonescu-Cuypers, C.P., Harris, A., Wilson, R., Kagemann, L., Mavroudis, L.V., Topouzis, F., Coleman, A.L., 2004. Reproducibility of the Heidelberg retinal flowmeter in determining low perfusion areas in peripapillary retina. Br. J. Ophthalmol. 88, 1266–1269.
Kjer, P., 1959. Infantile optic atrophy with dominant mode of inheritance:a clinical and genetic study of 19 Danish families. Acta Ophthalmol. Suppl. 164 (Supp 54), 1–147.
Kraus, M.F., Liu, J.J., Schottenhamml, J., et al., 2014. Quantitative 3D-OCT motion correction with tilt and illumination correction, robust similarity measure and regularization. Biomed. Opt. Express 5, 2591–2613.

Liu, L., Jia, Y., Takusagawa, H.L., et al., 2015. Optical coherence tomography angiography of the peripapillary retina in glaucoma. JAMA 133 (9), 1045–1052.
Newman, N.J., 2005. Hereditary optic neuropathies. In: Miller, N.R., Newman, N.J., Biousse, V., Kerrison, J.B. (Eds.), Walsh and Hoyt's Clinical Neuro-Ophthalmology, sixth ed. 1. Lippincott Williams & Wilkins, Philadelphia, PA, pp. 465–501.
Nikoskelainen, E., Hoyt, W.F., Nummelin, K., 1983. Ophthalmoscopic findings in Leber's hereditary optic neuropathy: II. The fundus findings in the affected family members. Arch. Ophthalmol. 101, 1059–1068.
Rao, H.L., Kadambi, S.V., Weinreb, R.N., et al., 2016a. Diagnostic ability of peripapillary vessel density measurements of optical coherence tomography angiography in primary open-angle and angle-closure glaucoma. Br. J. Ophthalmol. [Epub ahead of print].
Rao, H.L., Pradhan, Z.S., Weinreb, R.N., et al., 2016b. Regional comparisons of optical coherence tomography angiography vessel density in primary open-angle glaucoma. Am J. Ophthalmol. 171, 75–83.
Rönnbäck, C., Grønskov, K., Larsen, M., 2014. Retinal vessel diameters decrease with macular ganglion cell layer thickness in autosomal dominant optic atrophy and in healthy subjects. Acta Ophthalmol. 92 (7), 670–674.
Wang, X., Jia, Y., Spain, R., Potsaid, B., Liu, J.J., Baumann, B., Hornegger, J., Fujimoto, J.G., Wu, Q., Huang, D., 2014. Optical coherence tomography angiography of optic nerve head and parafovea in multiple sclerosis. Br. J. Ophthalmol. 98 (10), 1368–1373 October.
Wang, X., Jiang, C., Ko, T., et al., 2015. Correlation between optic disc perfusion and glaucomatous severity in patients with open-angle glaucoma: an optical coherence tomography angiography study. Graefes Arch. Clin. Exp. Ophthalmol. 253, 1557–1564.
Yaoeda, K., Shirakashi, M., Funaki, S., Funaki, H., Nakatsue, T., Abe, H., 2000. Measurement of microcirculation in the optic nerve head by laser speckle flowgraphy and scanning laser Doppler flowmetry. Am J. Ophthalmol. 129, 734–739.
Yarmohammadi, A., Zangwill, L.M., Diniz-Filho, A., et al., 2016. Relationship between optical coherence tomography angiography vessel density and severity of visual field loss in glaucoma. Ophthalmology 123, 2498–2508.
Yarosh, W., Monserrate, J., Tong, J.J., et al., 2008. The molecular mechanisms of OPA1-mediated optic atrophy in drosophila model and prospects for antioxidant treatment [report online]. PLoS Genet. 4, e6 Available at:. http://www.plosgenetics.org/article/info%3Adoi%2F10.1371%2Fjournal.pgen.0040006 (Accessed November 18, 2009).
Yu-Wai-Man, P., Griffiths, P.G., Burke, A., et al., 2010. The prevalence and natural history of dominant optic atrophy due to OPA1 mutations. Ophthalmology 117 (8), 1538–1546.
Yu-Wai-Man, P., Griffiths, P.G., Chinnery, P.F., 2011. Mitochondrial optic neuropathies-disease mechanisms and therapeutic strategies. Prog. Retin. Eye Res. 30 (2), 81–114.